Responses to reviewer #2

Dear Editor and Reviewer #2:

We greatly appreciate your consideration and the reviewer's insightful and constructive comments on the manuscript "Optimizing Ammonia Emissions for $PM_{2.5}$ Mitigation: Environmental and Health Co-Benefits in Eastern China" (egusphere-2025-1407). We have carefully revised the manuscript to address all the comments described below. Reviewer comments are shown in blue. Our responses are shown in black. The revised texts are shown in red.

Major comments:

1. Although the authors do not mention, it seems to me that the MLR-based approach assumes a linear relationship between NH_3 emissions and column concentrations and attributes all discrepancies between satellite observed and simulated NH_3 columns to local NH_3 emissions. It is important for the authors to clarify these assumptions and discuss the associated uncertainties. Specifically, (1) How might the nonlinear response of NH_3 concentrations to emissions affect the results? For example, do the summed contributions from individual sources ($SA_{agriculture}$ + $SA_{non\text{-}agriculture}$ + $SA_{transport}$) approximate the simulated total NH_3 column from the prior? (2) To what extent could transport of emissions from nearby grid cells influence the posterior results and cause spatial misattribution of emissions? (3) How might uncertainties in emissions of other pollutants (e.g., SO_2, NO_x) or in the model's representation of inorganic aerosol formation, impact the posterior estimates of NH_3 emissions? Could the large discrepancies between prior simulated and observed NH_3 column concentrations due to these factors? Some quantitative discussion or sensitivity analysis on these points would help strengthen the credibility of the posterior estimates.

Response:

(1) We thank the reviewer for this insightful question. We acknowledge that the relationship between NH_3 emissions and atmospheric concentrations is inherently non-linear. Ambient SO_2 and NO_x lead to rapid gas-to-particle partitioning, indicating that a significant portion of newly emitted NH_3 is quickly converted to particulate ammonium. This "buffering effect" results in the non-linear response of the gaseous NH_3 column to emission changes.

In this study, the WRF-Chem-based iterative algorithm we employed, while

utilizing multiple linear regression at each iteration step, is capable of capturing the nonlinear characteristics of NH_3. Specifically, (1) the WRF-Chem model dynamically simulates the nonlinear chemical process governing the response of NH_3 column to emission changes during each linear iteration step; and (2) the collective behavior of these multiple linear iterations enables the representation of the overall nonlinear characteristics. As shown in Figure R2.1, by plotting intermediate results from ten regression iterations of non-agricultural emission adjustments over the study region during autumn, we demonstrate non-constant emission adjustment factors and non-proportional concentration responses, empirically confirming our algorithm's capacity to resolve non-linear atmospheric feedbacks.

Regarding the additivity of concentration responses raised by the reviewer, we acknowledge that the sum of NH_3 columns from individual source simulations (i.e., $SA_{agriculture} + SA_{non\text{-}agriculture} + SA_{transport}$) deviates from the total column simulated with combined prior emissions. This discrepancy (5.4%–15.7%) is a consequence of the non-linear chemical feedback within the atmospheric system. To ensure methodological consistency, we explicitly state that all evaluations and satellite-based comparisons exclusively use results from simulation with the unified posterior emission inventory, avoiding any summation of segmented source contributions.

We have incorporated these clarifications into the manuscript to make our methodology and its approach to handling the system's non-linearities clearer for the reader.

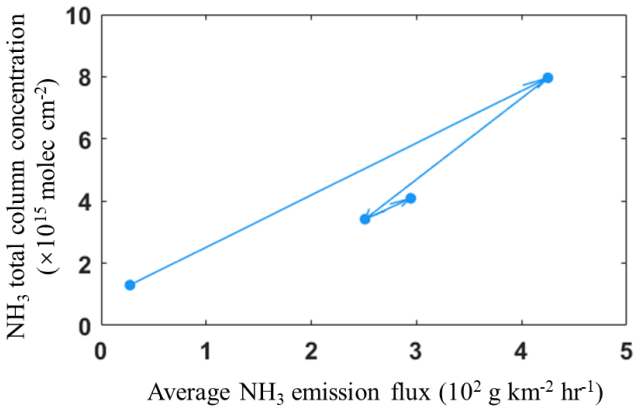

Figure R2.1. Scatter plot of NH_3 total column concentration versus NH_3 emission intensity for several steps of the iterative process. Arrows indicate the sequence of iterations.

(2) Thank you for pointing this out. To quantitatively address your concern about the potential spatial misattribution of emissions due to transport, we conducted a sensitivity experiment to evaluate the transport impact of NH_3 from upstream regions on the NH_3 column concentrations in downstream regions. We focused our analysis on July, a month with high NH_3 concentrations, and selected the Yangtze River Delta (YRD) region as the representative upwind source area.

The sensitivity experiment includes two simulations using posterior emissions. One simulation runs with all emissions included, and the other runs in which the NH_3 emissions from the YRD region were zeroed out. By comparing these two simulations, we can quantify the contribution of YRD emissions to NH_3 column concentrations in the downstream region through transport.

As shown in Figure R2.2, the transport contribution in regions closely adjacent to the YRD border is approximately 15%. However, the average contribution from the YRD to the broader downwind area was found to be 3.8%, indicating that the limited influence of regional transport. To clarify this point, we have expanded the discussion of transport-related uncertainty in the manuscript.

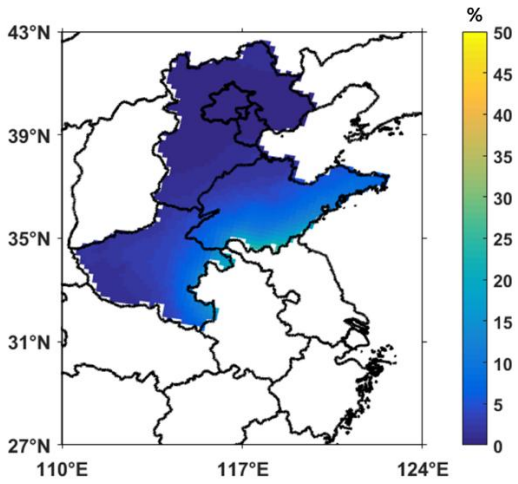

Figure R2.2. Transport contribution from the YRD region to NH_3 column concentrations in downstream study areas in July.

(3) Thank you for your comment. We show the comparison between the simulated SO_2 and NO_2 against surface observations from 80 sites across 9 cities in Table 3. The model presents a good performance in reproducing the concentration levels of these

precursors both in prior and posterior simulations. To further discuss the model's capacity in characterizing concentrations of secondary inorganic aerosols (SIA), we conducted comparisons using in-situ measurements at a representative site in Beijing (39°59′21″N, 116°18′25″E).

The evaluation results are summarized in Table R2.1. It is revealed that the posterior NH_3 emissions increase NH_4^+ concentration from 4.71 μg m^{-3} to 4.95 μg m^{-3}, which is closer to the observed average (5.69 μg m^{-3}). The simulated mean NO_3^- concentration with 9.59 μg/m³ also better matches the observed level (9.44 μg m^{-3}).

The WRF-Chem model performs moderately well in capturing the observed SO_4^{2-} concentration (7.74 μg m^{-3}) in both simulations (5.81-5.84 μg m^{-3}). The model underestimation could be attributed to the missing formation mechanism of sulfate such as transition metal ions (TMI)-catalyzed and photosensitized oxidation of SO_2 on aerosol surfaces (Cai et al., 2024; Wang et al., 2021, 2020). Although this underestimation of sulfate might lead to our posterior NH_3 emission estimates being conservatively low, we find that the model still reproduces the total secondary inorganic aerosol (SIA) concentrations well, with an overall bias of only -11.0%. This good performance in simulating the total aerosol sink for ammonia suggests that the uncertainty propagated to the final emission estimates from these chemical pathways is slight.

Table R2.1. Comparison between the prior and posterior simulated inorganic aerosol concentrations with in-situ measurements in Beijing. All value units are μg m^{-3}.

	Prior simulation	Posterior simulation	observation
nitrate	8.82	9.59	9.44
ammonium	4.71	4.95	5.69
sulfate	5.81	5.84	7.74

Regarding whether these factors (the emission for SO_2 and NO_x and the model's representation of inorganic aerosol formation) could be the primary cause of the large prior discrepancy, we conclude that while they introduce uncertainty, the systematic underestimation of NH_3 emissions is the principal driver. The prior simulation systematically underestimated the mean NH_3 column over Eastern China by 61%. Uncertainties in the emission inventories of other pollutants, such as SO_2 or NOx, or

biases in the chemical mechanisms, are insufficient to explain such a large and widespread systematic underestimation of NH_3 itself.

Furthermore, a key point of our study design is that the only variable adjusted between the prior and posterior simulations was the NH_3 emission inventory. This single adjustment led to significant improvements across multiple metrics. The model performance improved for concentrations of NH_3 and other relevant pollutants, such as SO_2, NO_2 and $PM_{2.5}$, indicating that NH_3 emissions were the core issue. In addition, previous studies have suggested that the bottom-up inventories frequently underestimated NH_3 emissions (Chen et al., 2021; Ding et al., 2024; Kong et al., 2019; Zhang et al., 2017). Overall, we would like to thank for your scientific suggestion and we have comprehensively revised the relevant content in the manuscript to make our statement and discussion clearer.

Revision in Section 2.2:

Furthermore, speciated inorganic aerosol data from a representative site in Beijing were collected to evaluate the model's capacity in characterizing the formation of secondary inorganic aerosols (Tan et al., 2018).

Revision in Section 4.1:

Finally, the entire process is iteratively repeated, a framework that captures the overall non-linear atmospheric response by combining the dynamic simulation of non-linear chemistry within each WRF-Chem step with the collective behavior of multiple iterations.

Revision in Section 4.2:

Additionally, uncertainties from the model's chemical mechanisms and the influence of nearby grid transport also contribute to this gap, but the overall impact on the final estimate is limited.

Revision in Section 4.3:

To further characterize the model's chemical performance beyond total $PM_{2.5}$, we also evaluated the simulation of secondary inorganic aerosol (SIA) components against in-situ measurements from a representative site in Beijing (Table S7). The evaluation shows that the posterior NH_3 emissions improved the simulation of ammonium and nitrate, reducing the bias between simulated and observed concentrations. Although the model underestimates sulfate, likely due to missing formation mechanisms (Cai et

al., 2024; Wang et al., 2021, 2020), the total SIA concentration is well reproduced with an overall bias of only -11.0%.

Revision in Supplementary:

Table S7. *Comparison between the prior and posterior simulated inorganic aerosol concentrations with in-situ measurements in Beijing. All value units are μg* m^{-3}.

	Prior simulation	*Posterior simulation*	*observation*
nitrate	*8.82*	*9.59*	*9.44*
ammonium	*4.71*	*4.95*	*5.69*
sulfate	*5.81*	*5.84*	*7.74*

2. It is not very clear to me how the current MLR framework can separate AGR and non-AGR NH_3 emissions. Some clarification would be helpful, as noted in the minor comments below. Generally, in each grid cell j, I would expect the temporal variations in $SA_{agriculture}$ and $SA_{non\text{-}agriculture}$ to be perfectly correlated and differ only in magnitude, thus they could not be separated in the regression. While WRF-Chem may simulate different day-to-day variations for $SA_{agriculture}$ and $SA_{non\text{-}agriculture}$, that reflects the effects of transport from surrounding grid cells, which contradicts the assumption that transport effects are negligible. Also, it would be useful to explain why the emission corrections primarily affect the non-AGR sector. Given that non-AGR emissions are relatively small in the prior, one would expect $SA_{non\text{-}agriculture}$ to be much smaller than $SA_{agriculture}$ in Eqn (4). Is the regression coefficient b significantly larger than a, and if so, what is the reason for that? Specifically, in northern Henan, the posterior results show decreased AGR but increased non-AGR emissions compared to the prior, which seems hard to understand and needs further explanation.

Response:

We thank you for this insightful question regarding the separation of agricultural (AGR) and non-AGR sources within our MLR framework.

The effective separation of these two sectors in our study is primarily based on their distinct and inconsistent spatial distributions. The use of multiple linear regression (MLR) for source apportionment is a well-established approach in atmospheric science (Qi et al., 2024; Shu and Lam, 2011; Trošić Lesar and Filipčić, 2023) and can identify different physical sources. The fundamental principle of using regression for source

apportionment is that different sources can be statistically distinguished if they possess unique spatial "fingerprints".

In our study, the high-concentration regions resulting from AGR and non-AGR emissions do not spatially align (Figure R2.3). The overall spatial correlation between the NH_3 columns simulated from these two sources is low (r = 0.35) and is near zero in the high-concentration regions (r = 0.03). This significant dissimilarity provides a robust statistical basis for the MLR model to distinguish their relative contributions.

The adjustment of these sources occurs through a multi-stage iterative process. Initially, the algorithm addresses the large, domain-wide underestimation by increasing emissions from both sectors. In subsequent iterations, a finer adjustment occurs where the framework optimizes the relative mix of the two sources to better match the observed spatial patterns. This directly relates to the emission corrections. If the spatial pattern of non-AGR emissions provides a better fit to the remaining model-observation discrepancy in certain areas, its corresponding emissions will be increased more significantly. This can result in a larger effective adjustment for the non-AGR sector, even if its initial contribution is smaller.

The specific case of northern Henan, where AGR emissions decrease while non-AGR emissions increase, exemplifies this refinement stage. In this region, the initial emission adjustments likely resulted in a spatial pattern that did not perfectly match the satellite observations. The algorithm then corrects this by reducing the AGR sector's contribution while simultaneously increasing the non-AGR sector's influence, as the latter's spatial pattern provided a better fit. The success of this adjustment is quantitatively demonstrated by the significant improvement in model performance for this region: the spatial correlation in Henan increased from 0.47–0.58 in the prior to 0.64–0.90 in the posterior. This confirms the framework is effectively adjusting the relative structure of emissions to best match the observations.

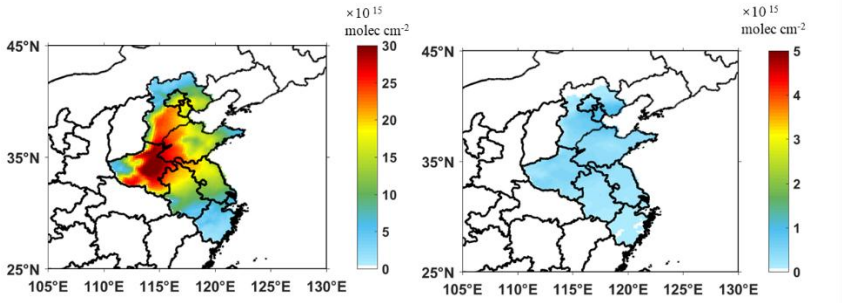

Figure R2.3. Spatial distribution of prior simulated NH_3 column concentrations from

agricultural and non-agricultural sources.

Revision in Section 4.1:

In each iterative calculation, the monthly average satellite-derived NH_3 column concentration served as the target, and multiple linear regression (MLR) was applied to calculate the corresponding regression factors for AGR and non-AGR emissions (Figure S3). This separation of sectors by MLR is effective because their respective spatial distributions are distinct and largely uncorrelated (r = 0.35).

Revision in Section 4.2:

In multiple iterations, the framework optimizes the relative mix of the two sources to better match the observed spatial patterns. For instance, the spatial correlation between model and observation in Henan increased from 0.47–0.58 (prior simulations) to 0.64–0.90 (posterior simulations).

3. The finding of substantially higher non-agricultural (non-AGR) NH_3 emissions compared to prior estimates is certainly interesting and important. However, the discussion of the posterior results in Section 4 currently focuses mainly on reporting emission magnitudes and sectoral contributions, with limited interpretation of the underlying causes or contextualization within existing literature. I would encourage the authors to expand this discussion by addressing the following points: (1) What are the potential reasons for the apparent underestimation of non-AGR NH_3 emissions in current bottom-up inventories? (2) What types of non-agricultural sources (e.g., industrial processes, transportation) are most likely responsible, based on current understanding? (3) How do your findings about non-AGR emissions compare with previous top-down estimates? The discussion in Lines 259–281 is helpful, but it could be further strengthened by emphasizing on observation-based or model-based studies that have investigated non-AGR NH_3 sources. It would also be valuable to highlight how your results build upon or differ from those studies, and what novel insights your analysis contributes to this topic.

Response:

(1) We thank the reviewer for the constructive suggestion The principle of bottom-up emission inventories is the product of activity level and emission factor. The accuracy of bottom-up inventories is highly dependent on the input data. However, incomplete activity levels, not representative emission factors, and the overlooked

sources make it a challenge to reasonably estimate non-AGR NH_3 emissions in China.

Several overlooked factors contribute to the underestimation of industrial NH_3 emissions in bottom-up inventories: (1) A significant source is "ammonia slip" from the widespread use of denitrification technologies (like SCR and SNCR) to control NO_x emissions. (2) a crucial and largely overlooked source is the 'indirect emission' of NH_3, where ammonia is first adsorbed onto byproducts like fly ash and desulfurization slurry and is subsequently released during their handling and utilization (Chen et al., 2022; Cheng et al., 2020; Liu et al., 2020). (3) emission inventories have often omitted a range of downstream chemical industries that use ammonia as a feedstock (Wei et al., 2022). The inclusion of these factors results in an estimate of industrial NH_3 emissions that is 3–10 times higher than those in previous bottom-up inventories (Chen and Wang, 2025).

Similarly, for residential sources, volatilization from landfills, wastewater treatment, and human excreta are important sources, especially in densely populated megacities. For example, some studies have identified human excreta as a stable and significant contributor to the urban NH_3 budget, a sector frequently omitted in traditional inventories (Chang et al., 2015; Shao et al., 2020).

For the transportation sector, many inventories rely on emission factors developed for European or U.S. vehicle fleets. These factors often fail to capture complex real-world conditions in China, such as catalyst aging, vehicle maintenance status, and diverse driving patterns in congested traffic. This leads to an underestimation of the true NH_3 emission rate, a finding confirmed by several field studies. (Chang et al., 2016; Sun et al., 2017; Zhang et al., 2021).

Underestimation across these multiple sectors demonstrates the systematic underestimation of non-AGR NH_3 emissions in current bottom-up inventories. We have rephrased the relevant texts in the manuscript for further discussion.

(2) We thank the reviewer for this insightful comment. We are unable to further categorize the posterior non-AGR emissions into specific sub-sectors due to two primary methodological limitations: (1) Introducing additional sub-sectors as separate factors in the Multiple Linear Regression (MLR) model would cause the results for some of these factors to become statistically insignificant. (2) At the current resolution of our model (18 km) and the prior emission inventory (0.25°), the spatial distributions of many non-AGR sub-sectors are too similar, which prevents our current method from

distinguishing between them. However, your comment offers us an excellent opportunity to discuss the current understanding of the relative importance of different non-agricultural sources based on existing literature.

We have compiled source apportionment results from several emission inventories in Figure R2.4. The inventories covering China suggests that, on a national scale, industrial and residential sources are two major contributors to non-agricultural NH_3 emissions. When we extract data specifically for our study domain from established grided inventories like MEIC and CEDS, with residential and waste-related sources showing significant contributions. This is confirmed by high-resolution inventories for sub-regions such as YRD, where residential and waste sources are also identified as primary contributors.

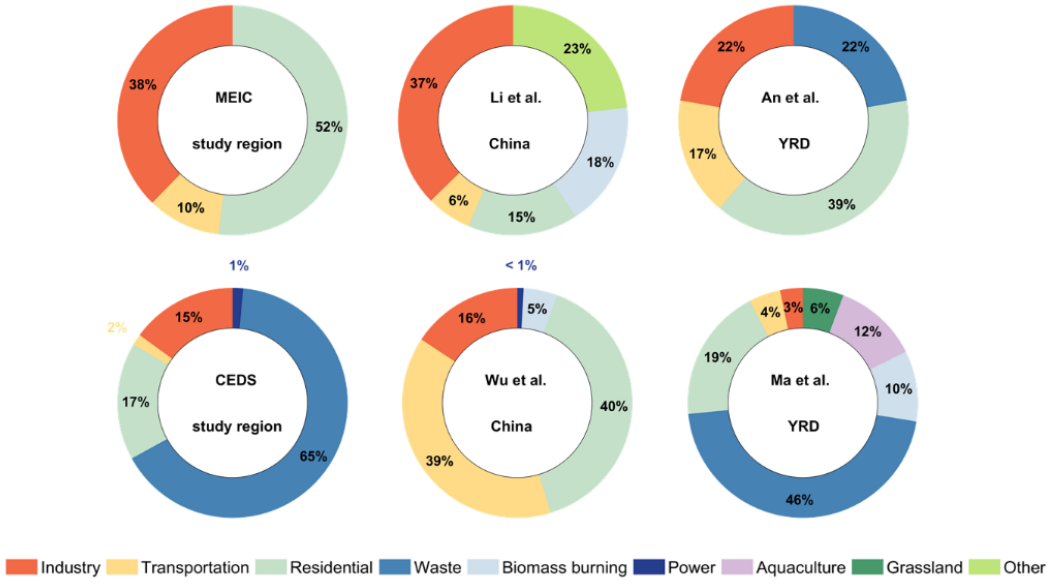

Figure R2.4. Comparison of the source apportionment of non-AGR NH_3 emissions from different studies and for various regions. Each pie chart illustrates the relative contribution (%) of nine specific non-agricultural sources, with the area (study region, China, and the YRD) and data source for each chart indicated in its center.

(3) We thank the reviewer for this suggestion. The majority of previous top-down studies on NH_3 have focused on optimizing the total emission budget, without explicitly separating the contributions from different sectors (Xu et al., 2023). Some studies attempted to qualitatively estimate source-specific NH_3 emissions. For instance, Kong et al. (2019) and Liu et al. (2022) used satellite-observed NH_3 hotspots and linked them

to specific industrial or agricultural point sources with external information (Kong et al., 2019; Liu et al., 2022). Other approaches have attempted a form of quantitative allocation by first using top-down methods to constrain the total emission, and then relying on the sectoral fractions from bottom-up inventories for further apportioning.

A separate and distinct approach involves the use of stable isotope analysis. These studies have provided crucial quantitative insights, suggesting that the contribution of non-AGR sources to ambient NH_3 concentrations can be remarkably high, potentially up to ~90% in specific urban environments (Pan et al., 2016; Wu et al., 2020). However, it is important to note that this valuable technique typically provides constraints on source contributions to ambient concentrations rather than directly on emission fluxes.

Our work builds upon these previous findings by attempting to quantitatively disentangle the emissions from agricultural and non-agricultural sectors directly within our top-down framework. Instead of optimizing the total emissions and then allocating them post-hoc based on bottom-up information, our iterative MLR approach uses the distinct spatial signatures of the two sectors to derive separate adjustment factors for each. This provides a direct, observation-based constraint on the relative contributions of AGR and non-AGR emissions over a large region.

This approach addresses a potential methodological gap in top-down research, which has traditionally faced challenges in achieving direct, quantitative source attribution at regional scales. While acknowledging the uncertainties and limitations inherent in our study, we suggest this methodology could offer a valuable pathway toward more effective utilization of satellite observations for investigating source-specific emission trends.

Revision in Section 4.2:

Analysis of emission inventories (An et al., 2021; Hoesly et al., 2018; Li et al., 2021, 2017; Ma, 2020; Wu et al., 2024) reveals that residential activities and waste disposal are dominant sources of non-AGR NH_3 emissions, particularly in densely populated regions (Figure S5).

The relatively small proportion of non-AGR emissions is likely due to overlooked industrial (e.g., NH_3 slip and indirect emissions) (Chen and Wang, 2025; Chen et al., 2022; Wei et al., 2022) and residential sources (e.g., from waste) (Shao et al., 2020), combined with unrepresentative transportation emission factors (Sun et al., 2017;

Zhang et al., 2021).

Our work attempts to quantitatively disentangle the emissions from AGR and non-AGR sectors directly within our top-down framework and facilitates a more comprehensive capture of neglected non-AGR sources.

Revision in Supplementary:

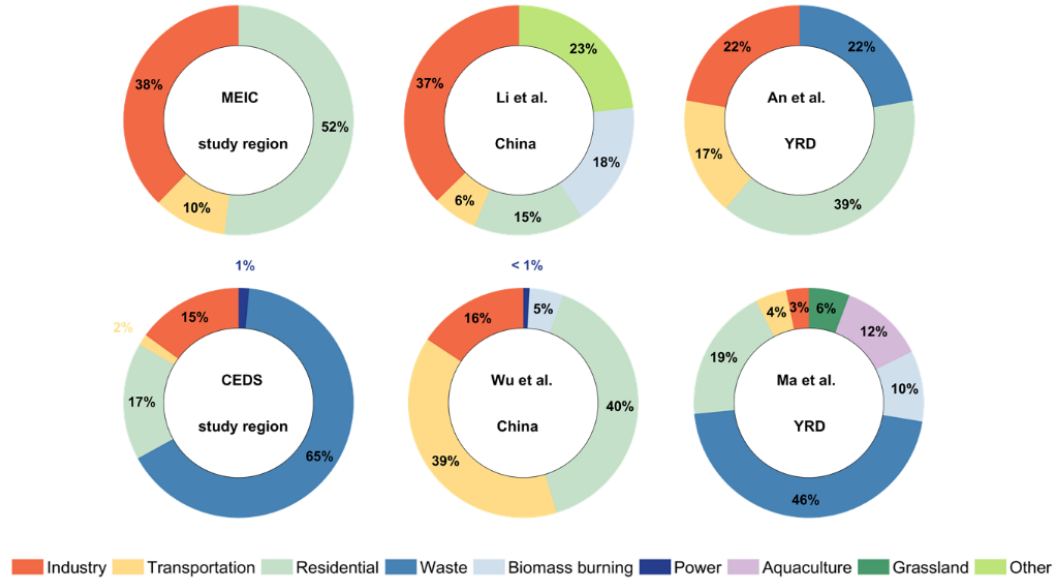

Figure S5. *Comparison of the source apportionment of non-AGR NH_3 emissions from different studies and for various regions. Each pie chart illustrates the relative contribution (%) of nine specific non-agricultural sources, with the area (study region, China, and the YRD) and data source for each chart indicated in its center.*

Minor comments:

1. Line 26/28 and elsewhere: please remove the "·" between Tg and yr^{-1}. Also, replace Gg mon^{-1} with either Gg $month^{-1}$ or Gg mo^{-1} to follow standard unit concentrations.

Response: Thank you for your careful reminder. We have checked that all expressions of emission units follow the standard format throughout the manuscript. Please refer to our revised manuscript.

2. Line 37-40. The summary statement is too general. It would be more informative to highlight the insights into non-agricultural ammonia emissions and their implications.

Response: Thank you for your comment. We have rephrased the relevant texts of the abstract to highlight the importance of identifying non-agricultural NH_3 emissions and their implications in reducing $PM_{2.5}$ pollution and health burden.

Revision in Section Abstract:

Our study evaluated NH_3 emissions from various sources in Eastern China, emphasizing the impact of reducing non-agricultural ammonia emissions on air quality and public health benefits.

3. Line 127: Is biomass burning emission also treated online? Just checking, as this is not commonly the case.

Response: Thank you for pointing this out. The biomass burning emissions were generated using the FINN v1.5, a model developed by NCAR. This model provided a useful utility for allocating the original wildfire emissions, which had a spatial resolution of 1km, to grid cells of the WRF-Chem model. Thus, we adopted an offline approach to prepare pollutant emissions from biomass burning. The description of this process in the previous manuscript contained inaccuracies. We have now revised the related section to reflect the correct methodology.

Revision in Section 2.1:

Furthermore, biogenic emissions were calculated online using the Model of Emissions of Gases and Aerosols from Nature (MEGAN, version 2.0.4) (Guenther, 2006). Our numerical simulations also incorporated offline biomass burning emissions of various air pollutants, based on the wildfire model Fire Inventory from NCAR (FINN, version 1.5) (Wiedinmyer et al., 2011).

4. Line 134: The “last accessed” date should reflect the actual date when the data were downloaded.

Response: Thank you for your kind reminder. The original IASI satellite products were actually downloaded in December of 2020. As you suggested, we have modified the statement regarding this data access date.

Revision in Section 2.2:

We obtained the total column density of NH_3 from the passive satellite remote-sensing product of the Infrared Atmospheric Sounding Interferometer (IASI) (version 3.0, https://iasi.aeris-data.fr/nh3/, last accessed on December 2020) as the observational constraint.

5. In section 2.2, what’s the overpass time of IASI data? Do you use level-2 satellite data?

Response: Thank you for this comment. IASI is a passive remote-sensing instrument that was first launched in 2006 on board the MetOp-A meteorological satellite, which circles the Earth in a polar Sun-synchronous orbit. It crosses the equator at mean local solar times of 9:30 and 21:30 (Van Damme et al., 2014), which are also the overpass times. In the present study, we used a processed satellite product at level 2 to access NH_3 column concentrations. We have revised the related text in Section 2.2 to better clarify the introduction of IASI data.

Revision in Section 2.2:

The IASI is a Fourier transform spectrometer on board the Metop series of meteorological satellites, which circle the Earth in a polar Sun-synchronous orbit (Van Damme et al., 2014). Consequently, the satellite-based IASI instrument can cover the entire globe and provide measurements twice a day at 09:30 and 21:30 local solar time. The IASI instrument detects infrared radiation in the spectral range from 645 to 2760 cm^{-1} emitted by Earth’s surface and atmosphere with a 12 km circular footprint at nadir. This radiation absorption range includes the NH_3 signal near 950 cm^{-1}. The collected daily NH_3 column concentrations are categorized into level-2 satellite data and are developed based on the ANNI-NH_3 inversion algorithm without averaging kernels, as presented by Van Damme et al. (2017).

6. Line 140-141: The description is unclear. How is the neural network applied to improve the data quality, was it developed by the authors or sourced elsewhere?

Response: Thank you for pointing this out. Van Damme et al. (2017) used the artificial neural network technique presented by Whitburn et al. (2016) to improve the quality of IASI satellite data. This work was carried out by other teams. Specifically, they trained separate neural networks for land and sea observations, resulting in a better training performance for both. To state this point clearer, we have rephrased the description of the IASI data product as follows.

Revision in Section 2.2:

The daily NH_3 column concentrations are categorized into level-2 satellite data and are developed based on the ANNI-NH3-v2.1 inversion algorithm without averaging kernels, as presented by Van Damme et al. (2017). Specifically, their retrieval algorithm derives hyperspectral radiation indexes (HRI) from the direct satellite spectrum detection, which is then converted into final NH_3 column concentrations using an artificial neural network technique (Whitburn et al., 2016). For better data quality, the present study removed NH_3 column concentrations associated with cloud cover of more than 10%. Furthermore, we preprocessed the IASI NH_3 column concentration data through averaging all daily values to obtain a monthly mean. Spatially, we mapped the original satellite product data to the grid cells of the WRF-Chem model for further comparison with those simulated NH_3 columns.

7. Line 125/156: Which version of MEIC is used?

Response: Thank you for your comment. Our study used version 1.3 of the MEIC anthropogenic emission inventory. We have included the version number in the revised manuscript as you suggested.

Revision in Section 2.1:

We adopted the anthropogenic emissions from the Multi-resolution Emission Inventory for China (MEIC, version 1.3) developed by Tsinghua University (Li et al., 2017; Zheng et al., 2018).

8. Line 162-163 and Section 4.1: Please clarify how the model and observations are sampled for comparison.

Response:

Thanks for your conducive comment. We conducted a model evaluation of NH_3 concentrations, comparing observations and simulations based on prior emissions, from two perspectives.

The first aspect is the total column concentration of NH_3. We calculated the respective simulated NH_3 column concentrations within 27 vertical layers. The overall NH_3 column concentration can then be inferred by summing up all the partial column concentrations. The IASI satellite data has been pre-allocated to the grid cells of the WRF-Chem model. We then sampled the monthly average total column concentration of NH_3 at the same grid cell, and carried out comparisons between IASI observations and WRF-Chem simulations.

Another validating parameter is the surface NH_3 measurement. In this circumstance, we only extracted the simulated NH_3 volume concentrations in the first layer near the ground surface. NH_3 measurements were collected from previous studies and are presented as annual averages (Table S2). Model simulations of NH_3 volume concentrations were sampled at certain grid cells according to the longitudes and latitudes of 12 different measurement sites. The final comparison was made in terms of the annual mean NH_3 volume concentration at these sites, between model simulation and in situ observations. To clarify this point, we have rephrased the relevant text in the revised manuscript.

Revision in Section 3:

We compared the prior model results with IASI NH_3 column concentration and surface NH_3 volume concentration observations. The detailed method for calculating NH_3 total column concentrations and surface volume concentrations from WRF-Chem is provided in Text S1.

Revision in Supplementary:

For surface NH_3 volume concentrations, we extracted the corresponding simulations at 12 sites summarized from previous in situ measurement studies and conducted a comparison between the model simulations and the measurements in terms of the annual mean NH_3 volume concentrations.

9. Line 179: The term “errors” is vague. Consider using clearer language such as “underestimated by 30%” or “biased low by 30%.”

Response: Thank you for your comment. Following your suggestion, we have rephrased the relevant text in Section 3 to make this point clearer.

Revision in Section 3:

Most simulated NH_3 total column concentrations are underestimated by more than 30% compared with the observed values by satellite with the associated RMSE exceeding 10×10^{15} molec cm^{-2}.

10. Line 181-189: Figure 6 can be described with the text here.

Response: Thank you for your suggestion. We indeed agree with you that Figure 6 should be introduced here to better depict the spatial distribution pattern of the observed and the simulated NH_3 column concentrations. We have revised the placement of figures as you suggested.

Revision in Section 3:

As illustrated in Figure 6, satellite-based observations reveal that the spatial high-value areas of NH_3 column are located at the junction of Henan, Shandong, and Hebei provinces. In contrast, the prior modeling results show that NH_3 column densities are more concentrated in Henan. This indicates a clear discrepancy in the spatial distribution of NH_3 column densities between the prior simulations and the observations.

11. Section 3: Please be consistent in the use of statistical metrics. RMSE is used for IASI comparisons, while IOA and MFB are used for surface observations. A brief explanation of why different metrics are applied, and what each evaluates, would be helpful.

Response: Thank you for pointing this out. In fact, we calculated all three evaluation metrics for comparisons between model versus measurements both in the total column concentration and surface volume concentration of NH_3. However, not all metrics are presented in the original manuscript. As you suggested, we have revised the relevant text in Section 3 by discussing all evaluation metrics to better elucidate the model performance.

Revision in Section 3:

As shown in Table S5, the annual average of NH_3 total column concentrations is simulated to be 17.4×10^{15} molec cm^{-2} for Eastern China, with a 61% underestimation of MFB compared to the observations from IASI satellite retrievals (29.0×10^{15} molec

cm^{-2}). The IOA between observations versus simulations is 0.72. The seasonal simulations of NH_3 concentrations also exhibit significant discrepancies with observations, especially in spring. Specifically, the simulated NH_3 total column concentration in Eastern China is only 13.2×10^{15} molec cm^{-2} in spring, with concentration in 67.5% of the study region being underestimated by more than 50%. These discrepancies are evidently exhibited in Figure 3. Most simulated NH_3 total column concentrations are underestimated by more than 30% compared with the observed values by satellite with the associated RMSE exceeding 10×10^{15} molec cm^{-2}.

Additionally, the comparison between the simulated and observed surface NH_3 volume concentrations also indicates a notable underestimation (Figure S2). The mean simulated surface NH_3 volume concentration over the study region is 6.3 μg m^{-3}, which is only half of the observation value (12.7 μg m^{-3}), with an IOA of 0.57 and an MFB of -61%, respectively (Table S5).

Revision in Supplementary:

Table S5. List of the evaluation metrics of NH_3 concentrations.

	The total column concentration (10^{15} molc cm^{-2})		*Surface volume concentration (μg m^{-3})*	
	Prior	*Posterior*	*Prior*	*Posterior*
Mean obs.	*29.0*		*12.7*	
Mean model.	*17.4*	*23.7*	*6.3*	*9.4*
IOA	*0.72*	*0.91*	*0.57*	*0.65*
MFB	*-0.61*	*-0.30*	*-0.61*	*-0.19*
RMSE	*13.9*	*7.9*	*9.1*	*7.3*

12. Line 195: You mention deriving posterior emissions for four months—how are prior/posterior simulations compared with observations across the seasons? Are the same scale factors applied to all three months in each season? Please clarify. Given that WRF-Chem simulations are available for the full year, it would be more consistent to derive monthly emissions for all 12 months, which should follow the same procedure and would not require much additional effort.

Response:

Thank you for this question, which allows us to clarify the details and rationale of our experimental design. To clarify, our prior and posterior simulations were indeed

conducted for the full 12 months of 2016. Seasonal comparisons with satellite observations were made using seasonal averages of both simulated and observed data. However, the emission adjustments were derived exclusively from four representative months (January, April, July, and October). For each season, we first calculated a posterior emission inventory for its representative month using the corresponding adjustment factors, then applied this result uniformly to all three months within that season.

Our primary reason for adopting the representative-month approach was to enable a robust independent validation of our results, which is a common practice in computationally intensive modeling studies (Qu et al., 2017; Xia et al., 2025; Xu et al., 2021). By constraining our emissions using only four months, the remaining eight months serve as an independent dataset against which we can evaluate the performance of our posterior inventory. The good performance of our posterior simulation (including 'non-training' months) provides strong evidence that the adjustments are not over-fitted to specific monthly conditions and that the resulting posterior emission inventory is effective for the entire season.

Second, the use of representative months is a reasonable approach for characterizing seasonal patterns. The representative months effectively capture the overall seasonal cycle, with the highest concentrations in summer and the lowest in winter. Furthermore, the NH_3 column concentration of each representative month is in good agreement with its corresponding three-month seasonal average, with the relative difference ranging from only 1.9% to 17.3%. This small discrepancy confirms that our method reliably represents the seasonal average.

Furthermore, conducting year-round simulations for emission adjustments would incur substantial computational costs, which is a critical practical constraint. Our study conducted more than 20 regression iterations to optimize emissions. Extending this process to 12 months would demand additional computational resources of ~14 model-years, representing an extremely resource-intensive undertaking for regional chemical modeling.

We have revised the methodology section to provide this comprehensive explanation.

Revision in Section 4.1:

The posterior emission inventory derived for each representative month was then

applied to all three months within its corresponding season to generate the full 12-month posterior inventory. This representative-month approach was adopted to allow for a robust validation against the full 12-month period, with the remaining eight months serving as an independent dataset, and to manage the substantial computational cost of the iterative process.

13. Line 200: In Line 138, you mentioned that IASI data were regridded to the model resolution, but here you refer to single-pixel comparisons, which is somewhat confusing. Please clarify how the satellite data were matched to model outputs.

Response: We greatly appreciate your careful comment. We agree that the term "single-pixel" is not an appropriate statement. In the present study, we preprocessed the level-2 IASI satellite data via mapping them to the grid cells of the WRF-Chem model for further comparison with those simulated NH_3 columns. We have revised this confusing term to make the text clearer. Please refer to our revisions as follows.

Revision in Section 4.1:

In each iterative calculation, the monthly average satellite-derived NH_3 column concentration served as the target, and multiple linear regression (MLR) was applied to calculate the corresponding regression factors for AGR and non-AGR emissions (Figure S3).

14. Line 202: What does "regression factor" refer to? Is it the same as the emission scale factor?

Response: Thank you for the question, which helps us to clarify our terminology. In our manuscript, the term "regression factor" refers to the coefficients (α and β) derived from the MLR analysis. These factors effectively function as scaling factors for the prior emissions. The purpose of this process is to adjust the magnitude of the emissions from each sector so that the resulting simulated NH_3 column concentrations better match the satellite observations. We have revised the text to use this terminology more consistently and have clarified the definitions to improve clarity.

Revision in Section 4.1:

Furthermore, the MLR approach provided regression coefficients $\alpha_i^{j,k}$ and $\beta_i^{j,k}$, which function as scaling factors, respectively correspond to AGR and non-AGR NH_3 emissions in month j from region k, within the i iteration.

15. Line 206: Is $TA_{satellite}$ the monthly average or the daily average of NH_3

concentrations?

Response: Thank you for pointing this out. The symbol $TA_{satellite}$ shown here indicates the monthly average of NH_3 column concentrations from IASI satellite products. To make this point clearer, we have revised the texts in Sections 2.2 and Section 4.1 as follows.

Revision in Section 2.2:

Furthermore, we preprocessed the IASI NH_3 column concentration data through averaging all daily values to obtain a monthly mean value.

Revision in Section 4.1:

where, $TA_{satellite}{}^{j,k}$ denotes the monthly average of total NH_3 column density retrieved from the IASI satellite data, and $SA_{transport}{}^{j,k}$, $SA_{agriculture}{}_{i-1}^{j,k}$ and $SA_{non-agriculture}{}_{i-1}^{j,k}$ stand for the simulated total column concentration of NH_3 contributed by AGR emissions, non-AGR emissions, and outside transportation, respectively.

16. Line 208: Should be "outside transportation, AGR emissions, non-AGR emissions, respectively".

Response: Thank you for the comment and the careful reminder. It is indeed that the order is reversed. We have revised this sentence in a correct order.

Revision in Section 4.1:

$SA_{transport}{}^{j,k}$, $SA_{agriculture}{}_{i-1}^{j,k}$ and $SA_{non-agriculture}{}_{i-1}^{j,k}$ stand for the simulated total column concentration of NH_3 contributed by outside transport, AGR emissions, and non-AGR emissions, respectively.

17. Line 211: The term "control emissions" is unclear. Do you mean emissions were zeroed out? Also, please replace "cycle" with "experiment."

Response: Thank you for your suggestions. We acknowledge that the term "control emissions" here is of confusing. We would like to express the meaning of forcing the corresponding NH_3 emissions to zero as you mentioned. Meanwhile, we also have replaced the "cycle" with "experiment". Please refer to our revisions below.

Revision in Section 4.1:

In each experiment, we zeroed out AGR emissions, non-AGR emissions and regional external emissions to obtain the corresponding NH_3 column concentrations.

18. Line 214: What is A_{blank} used for?

Response:

Thank you for this question. The A_{blank} case refers to a simulated NH_3 total column in which all anthropogenic emissions within the study domain were turned off. The purpose of this simulation was to establish a blank line concentration field, which represents the influence of the chemical boundary conditions provided to our model domain.

As described in our methodology, the NH_3 column concentration resulting from the A_{blank} run is then subtracted from the other sensitivity simulations (e.g., A_{agr}, $A_{non-agr}$) to isolate the specific contribution of each in-domain emission sector. While the magnitude of this blank line concentration is very small compared to the contributions from emissions within the domain, it is an essential step to ensure accurate source attribution. We have clarified the role and definition of the A_{blank} simulation in the revised manuscript.

Revision in Section 4.1:

Specifically, the modeling case A_{blank} refers to a simulated NH_3 total column in which all anthropogenic emissions within the study domain were zeroed out. The purpose of this simulation was to establish background concentrations, which represents the influence of the chemical boundary conditions provided to our model domain.

19. Line 203/216: Earlier you use k for month and j for region, but later this is reversed. Please ensure consistency throughout. Also, using "grid cell j" is clearer than "region j" or "area j."

Response: We greatly appreciate your careful review. The typographical error has been corrected in the manuscript. Given that our calculations and analysis are region-based, we feel that 'region j' is a more descriptive term for our methodology. We have also revised the text to ensure this term is used consistently.

Revision in Section 4.1:

Furthermore, the MLR approach provided regression coefficients $\alpha_i^{j,k}$ and $\beta_i^{j,k}$, which function as scaling factors, respectively correspond to AGR and non-AGR NH_3 emissions in month j from region k, within the i iteration.

20. Line 217: It is unclear why does the regression is derived mathematically imply it

needs to be corrected? Please clarify the motivation for adjusting the regression coefficients.

Response:

We thank the reviewer for this question, which addresses an important detail of our methodology.

While a standard MLR provides a mathematical best fit, this fit may not always be statistically robust, particularly when be influenced by outliers. Our motivation for the correction procedure is to ensure that only statistically significant and reliable regression results are used to update the emissions. This prevents introducing noise from unreliable fits into the iterative process, which could lead to unstable or non-physical solutions.

We implemented a quality control procedure based on the statistical significance of the prediction error. For each regression, we calculate the residual (the difference between the observed and predicted values). If the 95% confidence interval of this residual does not contain zero, the model's prediction error is considered statistically significant, and the regression result is flagged as unreliable. As illustrated in the figure provided in our response, outliers (in red) are identified using this method.

We have revised the methodology section of the manuscript to explicitly state this motivation and to provide a clear description of our quality control procedure.

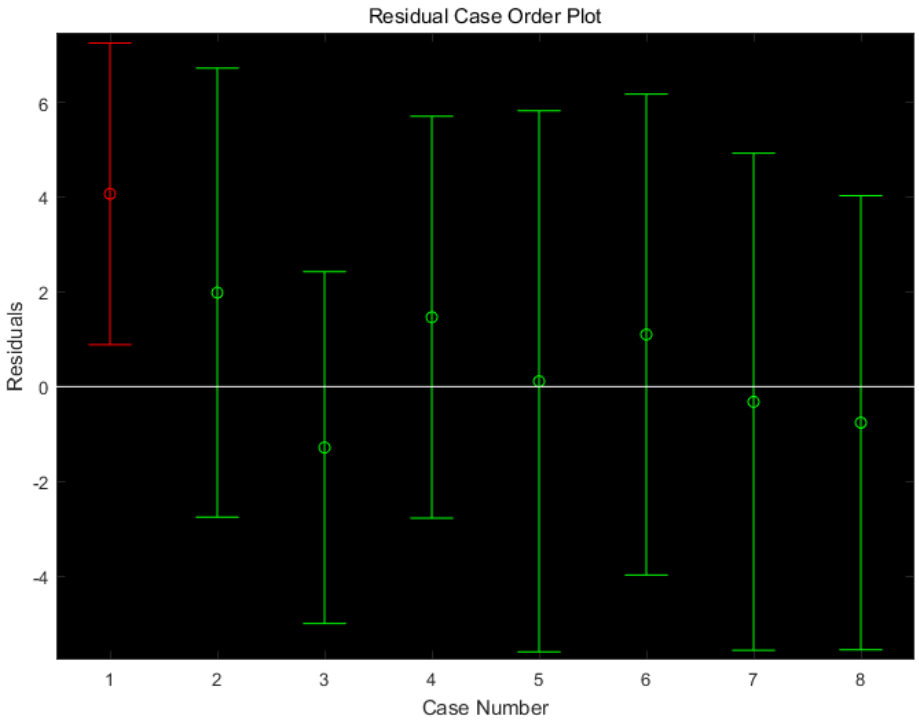

Figure R2.5： Distribution of residuals and their 95% confidence intervals. Each point represents the residual value for a given sample, and the error bars represent the 95% confidence interval of the residual. Green points represent valid fits, while red points are outliers rejected based on the criterion that their confidence interval does not contain zero.

Revision in Section 4.1:

To ensure the statistical robustness of the regression equation, we need to correct for this regression coefficient.

The regression coefficients with excessive residuals, defined as cases where the 95% confidence interval of the residual does not contain zero, are removed to increase credibility.

21. Line 218-231: The description of the correction process is not very clear. It is unclear what is meant by "goodness of fit," how the "invalid" regression coefficients are defined, and what fraction of them are removed. The phrase "make a trade-off" in Line 225 is vague and would benefit from clarification. Additionally, it is not explained how the adjustment factors a_n and b_n are derived or what their physical meaning is. The choice of a 30% threshold in Line 229 also seems arbitrary—particularly in high-NH_3 regions, where it could allow larger discrepancies between observations and simulations, but the physical basis for this threshold is not clearly explained.

Response:

The reviewer's meticulous feedback on our methodology is greatly appreciated, as it allows us to provide important clarifications. We have revised the manuscript to address these points in detail.

First, regarding the "goodness of fit" metric, we used the coefficient of determination (R-squared, R^2). A regression result was deemed "invalid" if the R^2 was less than 0.3 or if the 95% confidence interval of its residual did not contain zero. This is our quality control criterion for identifying and rejecting statistically poor fits. On average, 6.3% to 9.4% of regression results were rejected per iteration.

The phrase "make a trade-off" was used to describe our procedure for handling these invalid results. To clarify, if a regression result for a given grid cell is deemed

valid, the new adjustment factors (a and b) are set to the newly calculated regression coefficients (α and β). If the result is invalid, the adjustment factors are kept unchanged from the previous iteration ($a_i = a_{i-1}$).

This conservative approach ensures that emissions are only updated based on statistically robust fits, rather than deleting any data. The physical meaning of these adjustment factors, a and b, is that they represent the scaling multipliers applied to the prior emissions of the AGR and non-AGR sectors, respectively, to better match the satellite observations in each iteration.

Our choice of the 30% threshold was based on two primary considerations: (1) Within the widely accepted 20%–50% error range for model performance benchmarks, (EPA, 2007; Huang et al., 2021, 2025; Zhao et al., 2017), we selected 30% as our criterion to account for the inherent uncertainties in both the WRF-Chem model and the IASI satellite data. (2) Compared to the prior bias of up to -61%, reducing this bias to within 30% represents a significant and meaningful improvement, which proves that our method has imposed an effective constraint on the emission inventory.

Revision in Section 4.1:

Concurrently, the goodness of fit of the regression is calculated as the coefficient of determination (R-square, R^2). To maintain algorithm stability, regressions with an R^2 less than 0.3 are deemed invalid and excluded from the emission update, as they exhibit insufficient explanatory power (indicating >70% unexplained variance) and introduce destabilizing noise into the adjustments. We further use it to make a trade-off for the regression coefficient. If a regression is valid, the adjustment factors a and b are set to the new regression coefficients; if invalid, the factors are kept unchanged from the previous iteration. The updated emissions for the next iteration are then calculated by multiplying the emissions from the previous step by these adjustment factors.

The iteration concludes when the mean bias between the simulated values and observations is less than 30%, a criterion chosen to represent a significant improvement over the large prior bias while falling within the range of widely accepted model performance benchmarks.

References

Cai, S., Liu, T., Huang, X., Song, Y., Wang, T., Sun, Z., Gao, J., and Ding, A.: Important Role of Low Cloud and Fog in Sulfate Aerosol Formation During Winter Haze Over the North China Plain, Geophysical Research Letters, 51, e2023GL106597, https://doi.org/10.1029/2023GL106597, 2024.

Chang, Y., Deng, C., Dore, A. J., and Zhuang, G.: Human Excreta as a Stable and Important Source of Atmospheric Ammonia in the Megacity of Shanghai, PLoS One, 10, e0144661, https://doi.org/10.1371/journal.pone.0144661, 2015.

Chang, Y., Zou, Z., Deng, C., Huang, K., Collett, J. L., Lin, J., and Zhuang, G.: The importance of vehicle emissions as a source of atmospheric ammonia in the megacity of Shanghai, Atmospheric Chemistry and Physics, 16, 3577–3594, https://doi.org/10.5194/acp-16-3577-2016, 2016.

Chen, P. and Wang, Q.: Underestimated industrial ammonia emission in China uncovered by material flow analysis, Environmental Pollution, 368, 125740, https://doi.org/10.1016/j.envpol.2025.125740, 2025.

Chen, Y., Shen, H., Kaiser, J., Hu, Y., Capps, S. L., Zhao, S., Hakami, A., Shih, J.-S., Pavur, G. K., Turner, M. D., Henze, D. K., Resler, J., Nenes, A., Napelenok, S. L., Bash, J. O., Fahey, K. M., Carmichael, G. R., Chai, T., Clarisse, L., Coheur, P.-F., Van Damme, M., and Russell, A. G.: High-resolution hybrid inversion of IASI ammonia columns to constrain US ammonia emissions using the CMAQ adjoint model, Atmospheric Chemistry and Physics, 21, 2067–2082, https://doi.org/10.5194/acp-21-2067-2021, 2021.

Chen, Y., Zhang, Q., Cai, X., Zhang, H., Lin, H., Zheng, C., Guo, Z., Hu, S., Chen, L., Tao, S., Liu, M., and Wang, X.: Rapid Increase in China's Industrial Ammonia Emissions: Evidence from Unit-Based Mapping, Environ Sci Technol, https://doi.org/10.1021/acs.est.1c08369, 2022.

Cheng, T., Zhou, X., Yang, L., Wu, H., and Fan, H.: Transformation and removal of ammonium sulfate aerosols and ammonia slip from selective catalytic reduction in wet flue gas desulfurization system, J Environ Sci (China), 88, 72–80, https://doi.org/10.1016/j.jes.2019.08.002, 2020.

Ding, J., Van Der A, R., Eskes, H., Dammers, E., Shephard, M., Wichink Kruit, R., Guevara, M., and Tarrason, L.: Ammonia emission estimates using CrIS satellite observations over Europe, Atmos. Chem. Phys., 24, 10583–10599, https://doi.org/10.5194/acp-24-10583-2024, 2024.

EPA: Guidance on the Use of Models and Other Analyses in Attainment Demonstrations for the 8-hour Ozone NAAQS, 2007.

Huang, L., Zhu, Y., Zhai, H., Xue, S., Zhu, T., Shao, Y., Liu, Z., Emery, C., Yarwood,

G., Wang, Y., Fu, J., Zhang, K., and Li, L.: Recommendations on benchmarks for numerical air quality model applications in China – Part 1: $PM_{2.5}$ and chemical species, Atmos. Chem. Phys., 21, 2725–2743, https://doi.org/10.5194/acp-21-2725-2021, 2021.

Huang, L., Zhang, X., Emery, C., Mu, Q., Yarwood, G., Zhai, H., Sun, Z., Xue, S., Wang, Y., Fu, J. S., and Li, L.: Recommendations on benchmarks for numerical air quality model applications in China – Part 2: Ozone and uncertainty analysis, Atmos. Chem. Phys., 25, 4233–4249, https://doi.org/10.5194/acp-25-4233-2025, 2025.

Kong, L., Tang, X., Zhu, J., Wang, Z., Pan, Y., Wu, H., Wu, L., Wu, Q., He, Y., Tian, S., Xie, Y., Liu, Z., Sui, W., Han, L., and Carmichael, G.: Improved Inversion of Monthly Ammonia Emissions in China Based on the Chinese Ammonia Monitoring Network and Ensemble Kalman Filter, Environ Sci Technol, 53, 12529–12538, https://doi.org/10.1021/acs.est.9b02701, 2019.

Liu, P., Ding, J., Ji, Y., Xu, H., Liu, S., Xiao, B., Jin, H., Zhong, X., Guo, Z., Wang, H., and Liu, L.: Satellite Support to Estimate Livestock Ammonia Emissions: A Case Study in Hebei, China, Atmosphere, 13, 1552, https://doi.org/10.3390/atmos13101552, 2022.

Liu, W., Wu, B., Bai, X., Liu, S., Liu, X., Hao, Y., Liang, W., Lin, S., Liu, H., Luo, L., Zhao, S., Zhu, C., Hao, J., and Tian, H.: Migration and Emission Characteristics of Ammonia/Ammonium through Flue Gas Cleaning Devices in Coal-Fired Power Plants of China, Environ. Sci. Technol., 54, 390–399, https://doi.org/10.1021/acs.est.9b04995, 2020.

Pan, Y., Tian, S., Liu, D., Fang, Y., Zhu, X., Zhang, Q., Zheng, B., Michalski, G., and Wang, Y.: Fossil Fuel Combustion-Related Emissions Dominate Atmospheric Ammonia Sources during Severe Haze Episodes: Evidence from (15)N-Stable Isotope in Size-Resolved Aerosol Ammonium, Environ Sci Technol, 50, 8049–56, https://doi.org/10.1021/acs.est.6b00634, 2016.

Qu, Z., Henze, D. K., Capps, S. L., Wang, Y., Xu, X., Wang, J., and Keller, M.: Monthly top-down NO_x emissions for China (2005–2012): A hybrid inversion method and trend analysis, JGR Atmospheres, 122, 4600–4625, https://doi.org/10.1002/2016JD025852, 2017.

Shao, S.-C., Zhang, Y.-L., Chang, Y.-H., Cao, F., Lin, Y.-C., Mozaffar, A., and Hong, Y.-H.: Online characterization of a large but overlooked human excreta source of ammonia in China's urban atmosphere, Atmospheric Environment, 230, 117459, https://doi.org/10.1016/j.atmosenv.2020.117459, 2020.

Sun, K., Tao, L., Miller, D. J., Pan, D., Golston, L. M., Zondlo, M. A., Griffin, R. J., Wallace, H. W., Leong, Y. J., Yang, M. M., Zhang, Y., Mauzerall, D. L., and Zhu, T.: Vehicle Emissions as an Important Urban Ammonia Source in the United States

and China, Environ Sci Technol, 51, 2472–2481, https://doi.org/10.1021/acs.est.6b02805, 2017.

Tan, T., Hu, M., Li, M., Guo, Q., Wu, Y., Fang, X., Gu, F., Wang, Y., and Wu, Z.: New insight into PM2.5 pollution patterns in Beijing based on one-year measurement of chemical compositions, Science of The Total Environment, 621, 734–743, https://doi.org/10.1016/j.scitotenv.2017.11.208, 2018.

Wang, W., Liu, M., Wang, T., Song, Y., Zhou, L., Cao, J., Hu, J., Tang, G., Chen, Z., Li, Z., Xu, Z., Peng, C., Lian, C., Chen, Y., Pan, Y., Zhang, Y., Sun, Y., Li, W., Zhu, T., Tian, H., and Ge, M.: Sulfate formation is dominated by manganese-catalyzed oxidation of SO2 on aerosol surfaces during haze events, Nat Commun, 12, https://doi.org/10.1038/s41467-021-22091-6, 2021.

Wang, X., Gemayel, R., Hayeck, N., Perrier, S., Charbonnel, N., Xu, C., Chen, H., Zhu, C., Zhang, L., Wang, L., Nizkorodov, S. A., Wang, X., Wang, Z., Wang, T., Mellouki, A., Riva, M., Chen, J., and George, C.: Atmospheric Photosensitization: A New Pathway for Sulfate Formation, Environ. Sci. Technol., 54, 3114–3120, https://doi.org/10.1021/acs.est.9b06347, 2020.

Wei, L., Zhang, H., Sun, C., and Yan, F.: Simultaneous estimation of ammonia injection rate and state of diesel urea-SCR system based on high gain observer, ISA Transactions, 126, 679–690, https://doi.org/10.1016/j.isatra.2021.08.002, 2022.

Wu, C., Wang, G., Li, J., Li, J., Cao, C., Ge, S., Xie, Y., Chen, J., Liu, S., Du, W., Zhao, Z., and Cao, F.: Non-agricultural sources dominate the atmospheric NH3 in Xi'an, a megacity in the semi-arid region of China, Sci Total Environ, 722, 137756, https://doi.org/10.1016/j.scitotenv.2020.137756, 2020.

Xia, J., Zhou, Y., Fang, L., Qi, Y., Li, D., Liao, H., and Jin, J.: South Asia ammonia emission inversion through assimilating IASI observations, https://doi.org/10.5194/egusphere-2024-3938, 20 January 2025.

Xu, J., Lu, M., Guo, Y., Zhang, L., Chen, Y., Liu, Z., Zhou, M., Lin, W., Pu, W., Ma, Z., Song, Y., Pan, Y., Liu, L., and Ji, D.: Summertime Urban Ammonia Emissions May Be Substantially Underestimated in Beijing, China, Environ. Sci. Technol., 57, 13124–13135, https://doi.org/10.1021/acs.est.3c05266, 2023.

Xu, M., Jin, J., Wang, G., Segers, A., Deng, T., and Lin, H. X.: Machine learning based bias correction for numerical chemical transport models, Atmospheric Environment, 248, 118022, https://doi.org/10.1016/j.atmosenv.2020.118022, 2021.

Zhang, Q., Wei, N., Zou, C., and Mao, H.: Evaluating the ammonia emission from in-use vehicles using on-road remote sensing test, Environmental Pollution, 271, 116384, https://doi.org/10.1016/j.envpol.2020.116384, 2021.

Zhang, X., Wu, Y., Liu, X., Reis, S., Jin, J., Dragosits, U., Van Damme, M., Clarisse, L., Whitburn, S., Coheur, P. F., and Gu, B.: Ammonia Emissions May Be Substantially Underestimated in China, Environ Sci Technol, 51, 12089–12096, https://doi.org/10.1021/acs.est.7b02171, 2017.

Zhao, Y., Zhou, Y., Qiu, L., and Zhang, J.: Quantifying the uncertainties of China's emission inventory for industrial sources: From national to provincial and city scales, Atmospheric Environment, 165, 207–221, https://doi.org/10.1016/j.atmosenv.2017.06.045, 2017.